IEEE Access
Multidisciplinary ⋮ Rapid Review ⋮ Open Access Journal

Received December 21, 2020, accepted January 4, 2021, date of publication January 20, 2021, date of current version February 2, 2021.

*Digital Object Identifier 10.1109/ACCESS.2021.3052994*

# Peak Reduction and Long Term Load Forecasting for Large Residential Communities Including Smart Homes With Energy Storage

**HUANGJIE GONG[1], (Student Member, IEEE), VANDANA RALLABANDI[2], (Senior Member, IEEE), MICHAEL L. MCINTYRE[3], (Senior Member, IEEE), EKLAS HOSSAIN[4], (Senior Member, IEEE), AND DAN M. IONEL[1], (Fellow, IEEE)**

[1]SPARK Laboratory, ECE Department, University of Kentucky, Lexington, KY 40506, USA
[2]GE Research, Niskayuna, NY 12309, USA
[3]ECE Department, University of Louisville, Louisville, KY 40292, USA
[4]EERE Department, Oregon Institute of Technology, Klamath Falls, OR 97601, USA

Corresponding author: Dan M. Ionel (dan.ionel@ieee.org)

This work was supported in part by the University of Kentucky, the L. Stanley Pigman endowment, and in part by the Power and Energy Institute of Kentucky (PEIK), including its utility partners TVA and LG&E and KU.

**ABSTRACT** Domestic load profiles in the residential sectors are being modified with the adoption of smart home management systems and solar generation. In addition, houses with rooftop PV behave like local generators, contributing to the growth of the penetration of PV energy. Hence, the demand for power is declining day by day. However, the increasing PV penetration causes technical challenges for the power system, such as the ''duck curve''. This can be addressed through home energy management (HEM) techniques including peak shaving, load shifting with smart home devices. In this regard, electric water heaters (EWH), with high thermal mass and being ubiquitous, are attractive and low-cost energy storage systems. In this article, a case study for one of the largest rural field smart energy technology demonstrators involving business, industries, and more than 5,000 residences, located in Glasgow, KY, US, is presented. Furthermore, a HEM system, which aims to minimize the total energy usage and peak demand by regulating the heating, ventilation, and air-conditioning (HVAC) systems, water heaters, and batteries, thereby benefiting both the utility and the consumer is proposed. This work also demonstrates the ability of EWH to provide ancillary services while maintaining customer comfort. The minimum participation rates for EWH and batteries are calculated and compared with respect to different peak reduction targets. Long term load prediction by considering different fractions of smart homes for the utility is also provided.

**INDEX TERMS** Battery energy storage system (BESS), demand response (DR), electric water heater (EWH), grid service, home energy management (HEM), home energy model, power system, smart home.

## I. INTRODUCTION

The concept of smart homes is one of the enabling ideas for building a pathway towards a sustainable power system in the future by facilitating the participation of every power generation entity. The futuristic smart homes not only integrate information technology but also provide the opportunity to incorporate other innovative technologies such as PV, smart devices, and energy storage. Due to such technological advancements, smart homes can enhance energy efficiency, and improve both stability and reliability by allowing owners to regulate electricity usage [1]–[3]. They can also change the operations of utilities by minimizing both energy usage and peak demand in the residences [4]–[7].

Smart homes reduce energy usage by lowering heating, ventilation, and air-conditioning (HVAC) demand via improved building insulation and usage of intelligent control techniques to automatically turn off idle devices [8]–[11]. Furthermore, smart homes have the authority to control the appliances according to the command from the utility [12].

The associate editor coordinating the review of this manuscript and approving it for publication was Alexander Micallef.

With the growth of solar PV penetration, smart homes act as prosumers by participating in the energy market [13]–[15].

Some technical challenges are associated with the high penetration of PV in the residences, one of which is the ''duck curve''. This phenomenon occurs when the net power demand fluctuates with a large deviation within a short period, typically during the hours between the afternoon and the evening [16]. For ensuring local voltage support, it is necessary to maintain a minimum generation of electricity by the utility plants. Hence, the reliability of the power system is compromised when the generation of power is minimized during the mid-day to allow high PV generation [17]. To match with the fast increasing power demand in the evening, high-cost high-ramp rate generators are required when PV generation becomes unavailable [18].

Ancillary services, such as those described in [19], are provided in order to enhance the capabilities of the electric power system. The addition of energy storage can alleviate the ''duck curve'' through load shaving, peak shifting, self-consumption of the local PV generation. Smart homes can be used as virtual energy storage by utilizing various thermal components such as the HVAC systems, electric water heater (EWH) for circumventing peak demand [20]. Residence can support the ancillary services with its energy flexibility, which depends on factors including the capacity of the HVAC system [21]. The aggregated HVAC systems can be used to improve power quality efficient in demand response [22]. At the aggregated level, the HVAC systems can be controlled in a sequential way to reduce the peak demand while maintaining the user comfort [23].

Electric water heaters are also capable of providing ancillary services due to the large thermal mass of the water tank, as well as their presence in most households [24], [25]. The EWH can preheat the water to a much higher temperature while assuring the safety with the help of mixing valve technology [26]. Most EWH manufacturers provide the CTA-2045 modules in their new products or offer refurbishments to enable real-time communication and control [27], [28]. Previous research published by the extended group of authors showed that a smart home may achieve comparable functionality with a smaller battery energy capacity, provided that special EWH and associated controls are incorporated in a hybrid energy storage system [29]. The article included a systematic sizing procedure for such a home-based hybrid energy storage system and modeled it with a co-simulation framework for building energy use and electric power flow in distribution systems. In previous research, EWHs were used to regulate the frequency in an electric power distribution system [30]. Another research study showed that the aggregated EWH load can be controlled to contribute to shifting the system peak load [31]. Communities with large penetration of controllable EWH have, in principle, the potential for providing ancillary services.

This article is a substantially expanded follow up of a previous conference paper by the same research group, which showed that the increasing penetration of PV and HEM changes the aggregated load at the community level in the long term [20]. This work studies the capability of EWH to realize peak reduction based on the experimental data from ultra smart homes (USH) in the SET project. Water heating schemes are proposed to achieve different peak reduction targets while guaranteeing the customer comfort. The minimum participation rates for EWH are calculated and compared with that of the BESS.

Accurate prediction of the long term load can help utilities to better design the capacities of the infrastructure. This article also studies the long term total load profile for the utility considering the trends for increasing percentages of smart homes and the PV penetration in the residential community. It is demonstrated that with an appropriate HEM system, the ''duck curve'' at the power system level can be alleviated even when PV penetration is fairly high.

For distributed energy resources, including the afore mentioned demand response (DR) controllable EWH and HVAC, PV generators, and battery energy storage systems, further studies are required in order to fill in the research gap, develop specific controls, and establish methodologies for optimal sizing and for systematically quantifying the benefits and improvements, as later showed in the current paper. The major contributions of the article include: 1) proposal of a HEM algorithm which mitigates the ''duck curve'' caused by high PV penetration in a large community utilizing the building thermal properties; 2) prediction of the long term residential load for a large community with new technology penetrations based on the experimental data from one of the largest field demonstrator in the rural US; 3) quantification of the capability of using EWH to provide ancillary services.

The arrangement of the following article is as follows. The technology demonstrator and analysis framework is introduced in Section II. The home energy usage modeling, and HEM algorithm is described in Section III. In Section IV, the aggregated electric energy storage including batteries and water heaters are studied. The case studies for peak power reduction and long term impact of technology penetration are presented in V and Section VI, respectively. The conclusions are drawn in Section VII.

## II. TECHNOLOGY DEMONSTRATOR AND ANALYSIS FRAMEWORK

This article utilizes the experimental data from Smart Energy Technologies (SET) project in Glasgow, KY, a city for which utility services are provided by the municipal Electric Plant Board (EPB) in partnership with the Tennessee Valley Authority (TVA) [32]. Currently, this project is one of the largest rural field demonstrators in the US with high efficiency. The proposed software framework is implemented to model this entire advanced community that includes residential, business, and industrial sectors. The model incorporates a HEM system that allows regulating the residential EWH, HVAC, and BESS to reduce the peak demand and energy usage.

Building upgrades along with controllable and highly efficient devices are employed by the residential homes studied in this SET project (Fig. 1). According to the current data, over 300 homes out of around 5,000 from Glasgow, KY, are participating in the project. As a consequence, around 600,000 kWh of energy is being saved annually. All the residences participating in this SET project receive measures to improve energy efficiency such as efficient HVAC systems, better insulation, etc. Due to such improvements, energy usage is reduced in some of the SET homes, although all of them are single-family houses with comparatively larger space. Furthermore, programmable WiFi-enabled thermostats, heat-pump EWH, and a residential BESS allow the SET homes to perform real-time HEM.

**FIGURE 1.** Aerial view of Glasgow, KY, the location of the studied SET, along with pictures of smart devices for home energy management: thermostat, EWH and BESS, which are programmable and enabled by WiFi or Ethernet. The data acquired has a resolution of up to 1 minute and is available for both home owners and the utility.

Although the total power demand of the Glasgow EPB service includes business, industrial, and residential sectors, the system modeling presented in this study mainly emphasizes the residential sector and the aggregated effects of regulating single SET homes. The residential community includes five types of houses: non-SET conventional homes, residences with **H**VAC, **E**WH, and **B**ESS control (HEB), the HEB house with improved **I**nsulation (HEB_I), and the HEB, HEB_I house with local solar **PV** panels (HEB_PV, HEB_I_PV), respectively, as illustrated in Fig. 2. Apart from Non-SET conventional homes, the rest of the four types are SET homes. The residences in the SET project work as controllable loads with the integration of smart devices, bi-directional communications, and integrated management. It allows the houses to interact with the grid dynamically, and improves the coordination; leading to load shifting, peak demand reduction, and energy saving. The ultra smart homes (USH) with the Solar Integration System (SIS) monitor the residential power flow and upload real-time data. The available data from 148 USHs includes the net power flow from the grid, the power and state-of-charge (SOC) of the BESS.

Another set of data with the daily power profile for more than 5,000 residences is provided by the utility. The data includes the electricity usage at 15-minute intervals for each

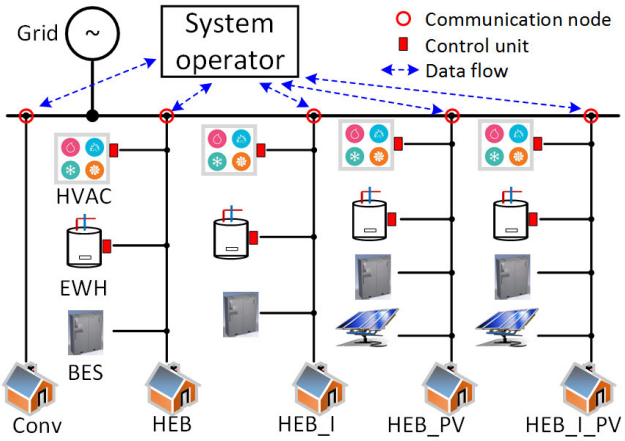


**FIGURE 2.** The proposed system model includes five types of SET homes, each type being representative of thousands of individual houses. In the study, the load data for the business and industrial sectors is provided by experimental measurements.

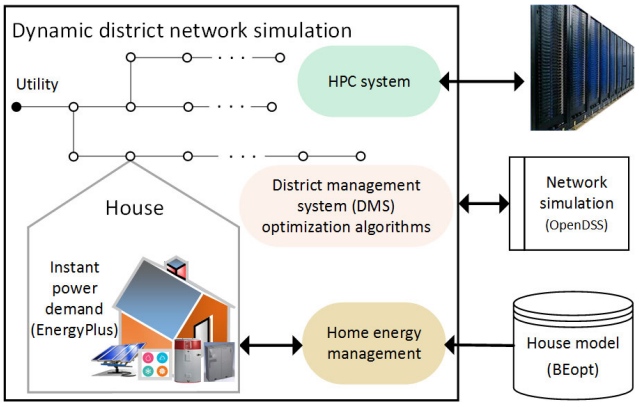


**FIGURE 3.** Schematic representation of the INSPIRE+D proposed simulation software framework, solely based on freeware, capable of running thousands of house energy models in parallel and concurrently performing power flow optimization.

individual home on example summer and winter days. The data serves as the baseline case, which presents typical power demand for the distribution system where most of the residences are conventional houses without PV. For the purpose of the computational study, the solar PV system for each house is sized in order to meet the NZE requirements, i.e. the energy used over one year has to be equal to the energy generated by the PV system.

The simulation for the power system formed by the SET community including over 5,000 homes is realized by an innovative, first of its kind, software framework '**I**ntegrated **N**etwork simulation for **S**mart **P**ower-flow **I**n **R**esidences using **E**nergyPlus and Open**DSS**' (INSPIRE+D), as shown in Fig. 3. INSPIRE+D incorporates freeware such as EnergyPlus, BEopt, OpenDSS, and Python, and is capable of both power flow analysis at the system level, and house energy modeling along with HEM at the single house level [29]. Its scalability allows the simulation of thousands of different house models in parallel, utilizing a high-performance computing (HPC) system with thousands of cores.

## III. HOME ENERGY MODELING AND MANAGEMENT

The net load for a residence with HEM_I_PV is the result of the combined power for HVAC, EWH, other loads, BESS, and PV, as illustrated in Fig. 4. The net load for a HEM house at time t is calculated as:

$$P_H^t = P_E^t + P_{HVAC}^t + P_O^t + P_B^t - P_{PV}^t, \quad (1)$$

where $P_H$ is the residential net power flow; $P_E, P_{HVAC}, P_O, P_B$ and $P_{PV}$ are the powers of the EWH, the HVAC system, other loads, the BESS and PV, respectively. It may be noted that for the BESS, positive and negative powers indicate charging and discharging, respectively.

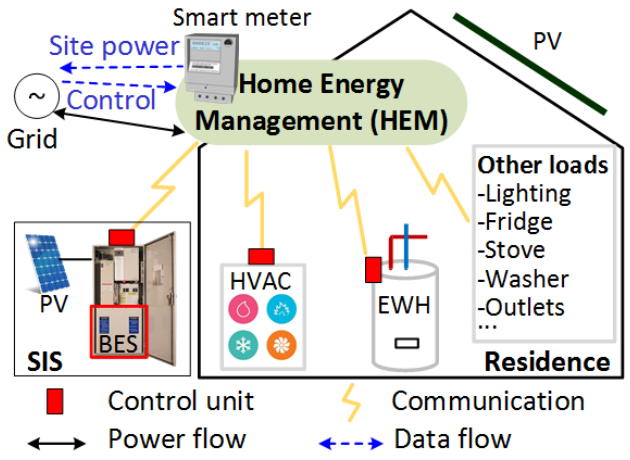


**FIGURE 4.** The proposed home energy management scheme for the SET homes. Solar PV and BESS are integrated into a Solar Integration System (SIS). HVAC and EWH load demands are controlled through temperature set points.

The water tank temperature is limited as follows,

$$T_S^t - \Delta T_D \le T_E^t \le T_S^t, \quad (2)$$

where $T_S$ is the set point of the EWH; $\Delta T_D$, the dead band of the EWH, which is set to 18F, $T_E^t$ the temperature of water in the EWH tank. $T_E^t$ is updated automatically by the house energy model. The water heater power is decided by the nominal power and its status from the following,

$$P_E^t = P_{E,N} \cdot S_E^t, \quad (3)$$

where $P_{E,N}$ is the nominal power of the EWH. The status of EWH, $S_E^t$, is decided by the water temperature in the tank, set points and the dead band as per the following,

$$S_E^t = \begin{cases} 0 = OFF, & T_E^t > T_S^t, \\ 1 = ON, & T_E^t < T_S^t - \Delta T_D, \\ S_E^{t-1}, & other. \end{cases} \quad (4)$$

The set point, $T_S^t$, for the EWH determines the required ON and OFF switching and the resultant power flow according to (2) – (4).

The high specific heat capacity of water, negligible heat loss, and mixing valves enable advanced controls, e.g., postponed electric heating load while sustaining the comfort of the consumers [33]. The effect of the EWH controls are exemplified in Fig. 5 for three EWH working schemes and their corresponding tank temperatures. Peak power due to EWH operation occurs in the morning without adopting any control mechanism. To avoid this morning peak, EWH is controlled to operate in the early morning and at midnight in the HEB-type homes without any PV generation system. The residences that include PV shift the EWH load to the afternoon to absorb the surplus PV generation.

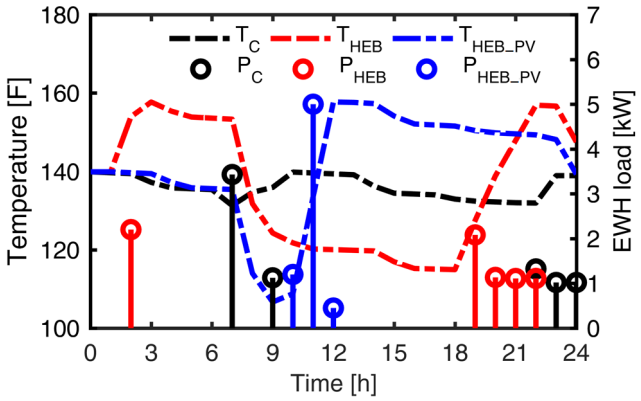


**FIGURE 5.** Water temperature in the tank and instantaneous power of EWH. HEB homes shift the EWH load to the morning and the evening. When equipped with solar PV, SET homes shift the EWH load to the afternoon to absorb surplus PV generation.

The HVAC power is represented as a function of the thermostat set point temperature change by the following,

$$P_{HVAC}^t = f(\Delta T_R^t). \quad (5)$$

Consumer comfort is taken into account by limiting the heating and cooling set points:

$$T_H^t \le T_R^{t-1} + \Delta T_R^t \le T_C^t, \quad (6)$$

where $T_R$, $T_H$, and $T_C$ stand for the room temperature, set points for heating and cooling, respectively. Previous research works show that the room temperature is influenced by factors including outdoor and ground temperatures, floor space, human activities and the heat radiation from indoor appliances [34].

The EnergyPlus software is employed to model the houses and quantify the results of the HVAC and EWH control. It may be noted that the user can over-ride the HEM controls if desired. The SET homes with the HEM system have lower HVAC loads on both the studied summer and winter days due to the improved insulation. The example control of HVAC in a winter day is presented in Fig. 6. By adjusting the mid-day temperature set point to a lower value, the HVAC power of the HEM house decreased significantly. In the afternoon when the SET house owner is away, the thermostat set point ($T_S$) is set low in order to reduce the HVAC load. $T_S$ is changed back at 17:00 before the house owner returns home.

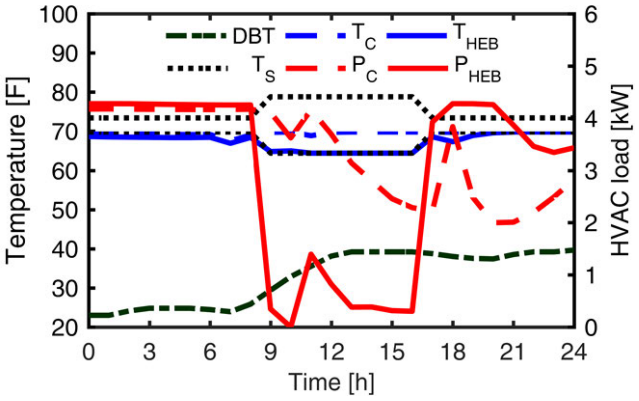


**FIGURE 6.** Simulated HVAC power demand for a typical home on an example winter day. A house of the conventional type (denoted by a suffix 'C') without HVAC control has higher HVAC power in the afternoon. In a HEB-type home, the capability of changing the heating set point ($T_S$), leads to lower HVAC power in the afternoon when the owner is away.

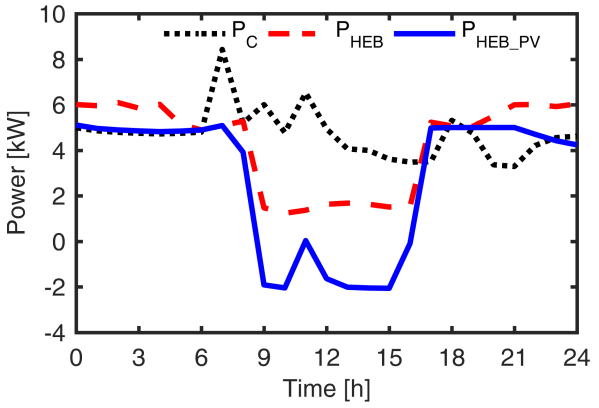


**FIGURE 7.** Simulated net power demand for a single-family house. The demands for HEB and HEB+PV houses are shaped by controlling the HVAC, EWH and BESS.

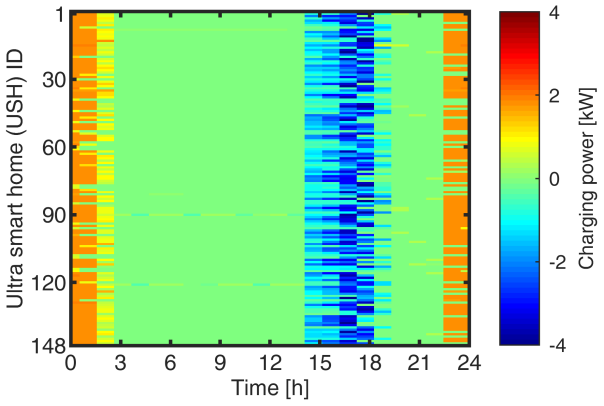


**FIGURE 8.** The BESS charging power for all the 148 ultra smart homes on the example summer day. The negative value in the afternoon indicates the BESSs are discharging. BESSs were charged in the middle of the night.

The net power flow of the NZE house is thus defined as a function of the HVAC set points, water heater set point, and the BESS power, as below,

$$P_H^t = f(P_B^t, T_S^t, T_H^t, T_C^t). \tag{7}$$

Based on the previous equations (1)-(7), and substantially following the concepts described in [35], a HEM algorithm has been developed and implemented at residence level in order to meet the power use limit set forth by the system operator utility via control signals during a DR event. Power in excess of the limit is firstly to be supplied, if available, by a BESS. Should such required supply exceed the maximum power of the BESS or should its state of charge be lower than admissible, appliances will be controlled to sequentially contribute to the power demand reduction, as briefly described in the following.

The energy used by the EWH will be reduced during DR by lowering the corresponding set point as exemplified in Fig. 5. In case the instantaneous power demand still exceeds the limit, the HVAC energy use is reduced by changing the set point for heating or cooling, depending on the season, as shown in Fig. 6. Changes may be performed incrementally until the utility-set upper power limit is meet and making sure, as a priority, that the minimum user comfort requirements are met.

The controllability of BESS provides enhanced flexibility to the HEM system because the charging and the discharging operations do not impact the comfort of the residents. The example effect of the BESS control from Fig. 7 illustrate the HEM functions for smoothing the residential energy demand and reducing peak power.

## IV. AGGREGATED ELECTRIC ENERGY STORAGE: BATTERIES AND WATER HEATERS

The data from all 148 USHs on an example summer day includes the power and SOC of BESS, and the net power flow from the grid for each house at 1-hour time-steps. In Fig. 8, the BESS measured power plotted during an example day is adapted to the typical use of electricity in the Southeast region [36], and includes charging periods at night, when the load is typically low, and discharging periods in the afternoon, during typical high demand. The experimental SOC data presented in Fig. 9 shows a maximum of 94% for all BESSs. There is only one single data point that is below 20%. Therefore, in this work, the maximum and minimum SOC of all the BESSs are regarded as 94% and 20%, respectively.

The SOC of most BESSs remained at the maximum until around 2pm. Corresponding to the BESS discharging operation, the SOC dropped to a minimum at 6pm. The BESSs were fully charged late at night, completing the operation cycle for a typical summer day. Based on the measured power and SOC for the BESS, BESS energy capacities for all 148 USHs are calculated and the average is 16.2kWh. The measured net power flow from the grid for each USH house in Fig. 10 shows that during the typical peak hours in the afternoon, almost all the USHs achieved near zero power due to controlled battery discharge operation. Also observed is the high power in the early morning and late night. Thus, it can be concluded that the BESS operation has a great impact on the net power flow at the system level.

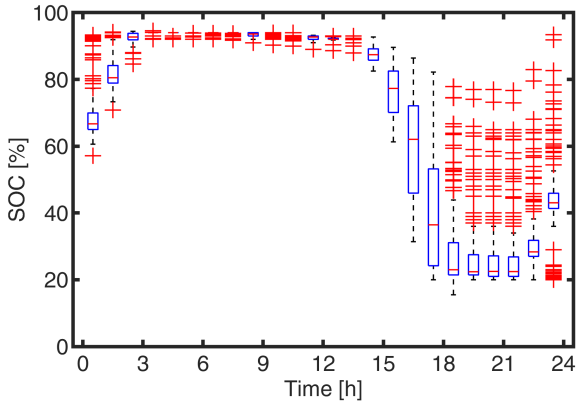


**FIGURE 9.** The SOC of BESSs from the 148 USHs on the example summer day. The measured data shows that the SOC could be regarded within [20%,94%]. The BESSs were charged in the middle of the night and maintained at the maximum SOC until around 2pm. The BESSs discharged for the afternoon peak and the low SOC remained until 9pm. The BESSs were charged afterwards and prepared for the next day.

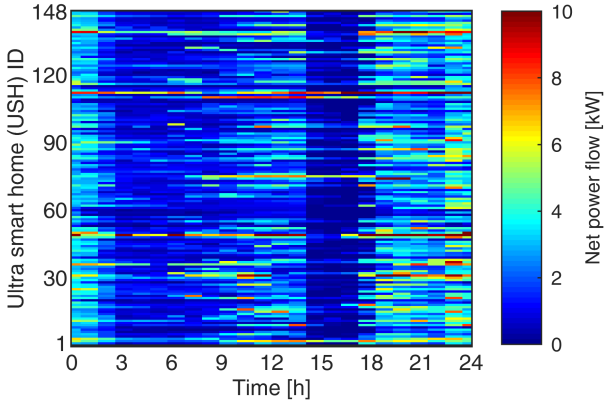


**FIGURE 10.** The net power from the grid for all the 148 USHs on the example summer day. The experimental data shows low net power at around 2pm–5pm. The power in the midnight was high due to BESS charging.

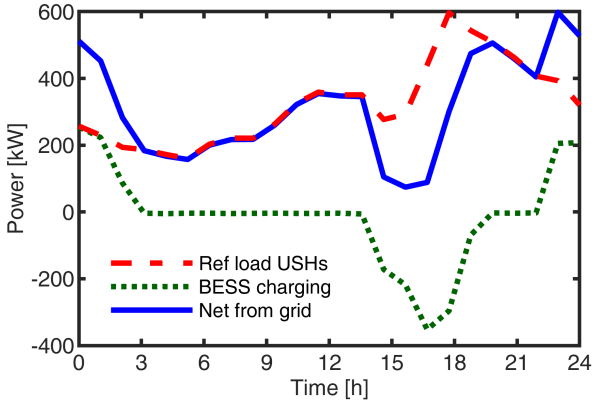


**FIGURE 11.** The aggregated power for all the 148 USHs based on the experimental data. The negative BESS charging power indicates the discharging operation at the peak hours. The aggregated net grid power at midnight was increased by the BESS charging.

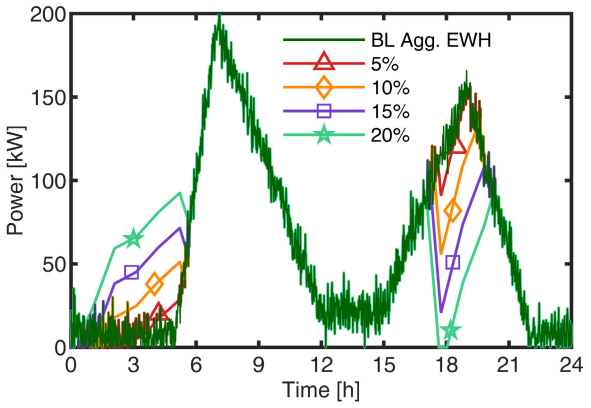


**FIGURE 12.** The power draw for EWH schemes including preheating and load shaving for different peak reduction targets labeled as percentage. The same amount of electricity for water heating was allocated at different times for the example day. The load shaving control was applied only to reduce the total evening peak.

The measured net power and BESS charging power for each of the USHs were added together to produce corresponding aggregated curves, as shown in Fig. 11. The curve labeled as Ref loads USHs represents the difference between the net grid power and BESS charging.

A new load aggregated curve corresponding to resistive EWHs was calculated and later used in the study to replace the experimental heat pump water heater loads. The aggregated resistive EWH load typically has morning and evening peaks, with an average peak power of around 1.5kW [37]. The aggregated EWH power-time curve can be substantially defined by its major turning points for which the mathematical derivative, i.e. ramping rate, changes drastically. In the example shown in Fig. 12 these turning points occur at approx. 5, 7, 12, 15, 19 and 22 o'clock. For example, a morning peak was exhibited around 7am, and a evening peak 7pm. The baseline (BL) aggregated EWH curve from Fig. 12 stands for the aggregated EWH power for all 148 USHs without power shaving. A white noise with signal-to-noise ratio of 20 was added to the BL curve. This value is based on the typical results reported by previous studies [37], which considered the naturally random user behavior on 75 different water heaters, which is approximately half the number of the units considered in our study.

A mixing valve technology allows the water temperature in the tank to be as high as 145F, increasing the thermal capacity of the EWHs. The hot water at the EWH exit is mixed with cold water in order to provide the user expected comfortable temperature. Four power shaving schemes were studied for different peak reduction targets and are shown in Fig. 12. The EWHs under all the schemes used the same amount of daily electricity and the same daily hot water draw. The peak shaving was realized by shifting the electricity used by EWH from the evening to the morning. It is worth noting that when the peak reduction target was 20%, the minimum aggregated EWH power was zero, meaning all EWHs were turned OFF during the peak period. It is possible that the 20% peak reduction target was not achieved even when all EWHs were turned OFF.

A first order equivalent EWH model was proposed to estimate the average water temperature in the tank for different

water heating schemes, as follows:

$$C\frac{\mathrm{d}\theta_T(t)}{\mathrm{d}t} = P(t) - \frac{1}{R}[\theta_T(t) - \theta_A] - \rho c_p W(t)\left[\theta_T(t) - \theta_{W,C}\right], \quad (8)$$

where $C$ is the equivalent capacitance, defined as follows:

$$C = V \cdot \rho \cdot c_p. \quad (9)$$

Other parameters are listed in Table 1.

**TABLE 1. Parameters for the Equivalent EWH Model.**

| Parameter | Value or unit |
|---|---|
| Density of water $\rho$ | 993 $^{kg}/_{m^3}$ |
| Specific heat capacity of water $c_p$ | 4,179 $^{J}/_{kg^\circ C}$ |
| Room air temperature $\theta_A$ | 22 °C |
| Temperature of cold water $\theta_{W,C}$ | 10 °C |
| Rated EWH heating rate $P$ | 4.5 kW |
| Water tank volume $V$ | 50 gallon |
| Equivalent resistance $R$ | 1500 $^{\circ C}/_{kW}$ |
| Water temperature in the tank $\theta_T$ | °C |
| Hot water draw $W$ | $m^3$/s |

It was assumed that the average tank temperature for the BL case is 125F at all time. With known power $P(t)$ and tank temperature $\theta_T(t)$ from the BL case, the daily hot water draw $W(t)$ is calculated by solving (8). The same daily hot water draw is used to calculate the average tank temperature for different water heating schemes shown in Fig. 12. The results in Fig. 13 show that when the water was preheated to a higher temperature in the morning, the EWH had more standby loss and lower temperature in the tank at the end of the day. Considering the benefits from peak reduction, the heat loss from preheating is worthwhile. In the case of 20% peak power reduction, the maximum average temperature reached approximately 140F, which can be realized through mixing valves. The lowest tank temperature for all the cases was 119F, which is satisfactory according to a study from the Department of Energy [38].

## V. REDUCTION OF PEAK POWER STUDY

In order to achieve higher peak power reduction, it is considered that all the heat pump EWH in the homes are replaced by equivalent resistive EWH. The Ref load USHs with the resistive EWH were calculated by subtracting the heat pump water heater load from the measured load data (Fig. 14). The heat pump load was estimated as a constant value of 20kW. The USH loads with EWH which represent the aggregated load for a community where all houses have resistive EWH, were calculated by adding the estimated equivalent aggregated resistive EWH load to the Ref load USHs curve from Fig.14.

The EWH power was shaved in the evening in order to reduce the peak demand, as shown in Fig. 15. The USH loads incl. EWH curve represents the baseline case where no peak reduction was applied. With peak reduction, the power in the evening was shifted to the morning. The aggregated water heating loads for different peak reduction targets were calculated in the previous section and presented in Fig. 12.

Ultra-smart homes can provide ancillary services by turning OFF the EWHs. The minimum participating rate of EWH

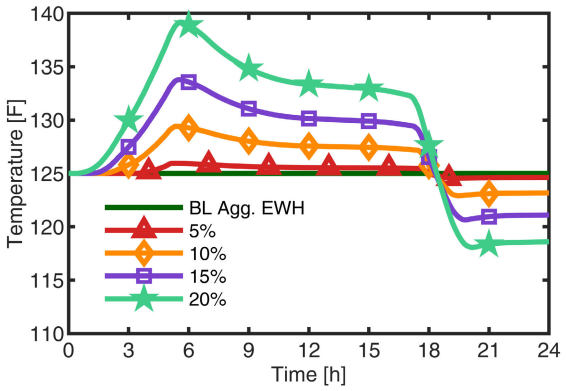


**FIGURE 13. The calculated average temperature for all the 148 USHs with different water heating schemes. Preheating in the morning led to higher temperature in the tank, resulting in more standby loss and lower tank temperature at the end of the day when the same amount of electricity was used for heating. Results show that the proposed heating schemes maintain the water temperature within the comfort and safety tolerances.**

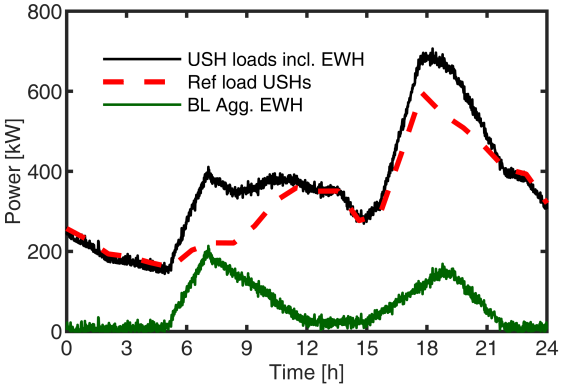


**FIGURE 14. The aggregated EWH and residential loads. The experimental heat pump water heater load in the Ref load USHs curve was replaced by the BL aggregated EWH curve. The curve of USH loads with EWH stands for the aggregated residential loads where all USHs used purely resistive EWHs.**

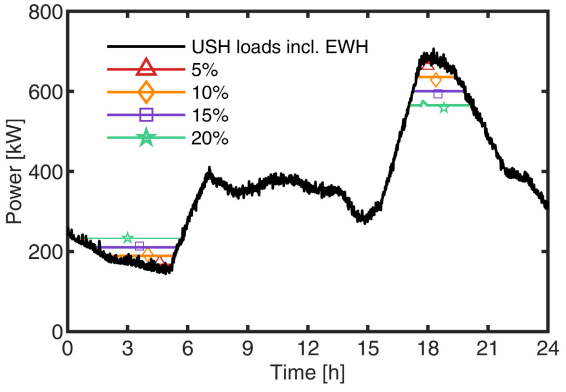


**FIGURE 15. The aggregated total USH loads with different water heating schemes. Peak reduction was realized by shifting the water heating load in the evening to the early morning. It is worth noting that shaving the EWH loads reduced the peak demand by approximately 18% maximum in this example, missing the real target of 20%.**

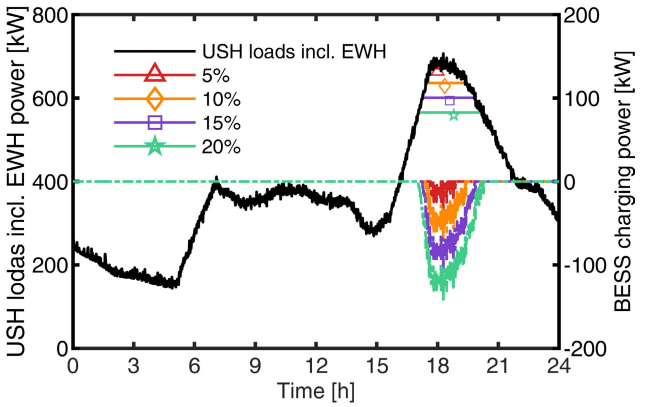


**FIGURE 16.** The aggregated total USH loads with peak reduction achieved by BESS. Only the discharge operation of BESS are shown.

was estimated with the average EWH power of 1.5kW during the peak time. The minimum participation rates for USHs to turn OFF EWH were 17%, 32%, 48%, 62%, for 5%, 10%, 15%, 20% peak reduction targets, respectively, as listed in Table 2. In the extreme case for 20% peak reduction target, even all the EWHs were turned OFF at the critical hour, the power was only reduced by 18%, missing the 20% target. This is due to the fact that EWH can only shave its own power but can not supply other loads, unlike BESS. With all the EWHs turned off, further reduction in peak power is not feasible. Even with these limitations, EWH is still an attractive candidates for providing ancillary services due to its near ubiquity and low additional cost.

The same peak reduction was achieved by the BESS and results are shown in Fig. 16. All the BESSs were charged during the late night and early morning. When the load shaving control process started, all BESSs had the maximum SOC. In Fig. 16, only the discharging power is plotted. With the BESS controlled to provide ancillary services, both the maximum power and available energy were taken into consideration. The BESS power was estimated 4.8kW with the nominal voltage of 48Vdc and charging rate of 100A. The average BESS energy capacity was 16.2kWh and the SOC can vary from 94% to 20%. Therefore, the BESSs have the capability to provide approximately 12kWh energy on an average.

With the peak reduction target set to 5%, a total energy of 12kWh and a maximum power of 30kW were needed to be provided by the BESS. At least seven USHs were required to provide a peak power of 30kW, even one BESS would be enough to provide the required energy of 12kWh. The shaved energy during the peak hour were 12kWh, 49kWh, 114kWh, 210kWh for 5%, 10%, 15%, 20% peak reduction targets, respectively. Meanwhile, the shaved power levels were 35kW, 70kW, 105kW, 134kW for the same peak reduction targets. Therefore, the minimum participation rates of BESS were decided by the shaved power as 6%, 11%, 15%, 21% for the peak reduction targets, respectively, as listed in Table 2.

It is shown that both BESS and EWH can provide ancillary services. Higher participation rates of EWH were required to realize the same peak reduction target. In this article, the maximum peak reduction achieved by the EWHs was 18% on the example summer day.

**TABLE 2.** The Minimum Requirement for USH Participation.

| Peak reduction target (%) | Shaved power target (kW) | BESS PART. (%) | EWH PART. (%) |
|---|---|---|---|
| 5 | 35 | 6 | 17 |
| 10 | 70 | 11 | 32 |
| 15 | 105 | 15 | 48 |
| 20 | 141 | 21 | 62 |

## VI. LONG TERM IMPACT OF TECHNOLOGY PENETRATION STUDY

In Table. 3, case studies based on different penetration of technologies, i.e., house types, are demonstrated. The experimental data provide the baseline case (BL) and stands for the current field situation where only around 300 out of around 5,000 homes are SET, and do not possess PV installations. In the second case, HEM control is not included. The net power flow curves of both the aggregated and the baseline case are similar, which validates the model. The improved insulation increases the efficiency of HEM_I homes, which causes a reduction in the total energy usage for case 2. Cases 2 to 5 present the gradual shift to futuristic high energy efficiency and distributed PV generation community. The simulation of the distribution power system for each case study was performed based on a modified IEEE 13-node test case, and solved by OpenDSS.

**TABLE 3.** Case Studies With Different Percentage Distributions of House Types in the Community Power System.

| Cases | Conv (%) | HEB (%) | HEB_I (%) | HEB_PV (%) | HEB_I_PV (%) |
|---|---|---|---|---|---|
| BL | >94 | <3 | <3 | 0 | 0 |
| 2 | 50 | 25 | 25 | 0 | 0 |
| 3 | 50 | 0 | 0 | 25 | 25 |
| 4 | 20 | 20 | 20 | 20 | 20 |
| 5 | 0 | 25 | 25 | 25 | 25 |

The case studies were performed on two preselected representative days in Glasgow, KY—1/19/2017 (Winter) and 7/20/2017 (Summer). In Fig. 17 (a), the aggregated residential power demand peaks in the morning and the evening on the winter day is shown. On this winter day, the residential load drops in the afternoon because of the solar irradiance, which brings heat into the room through walls and windows. The net power flow decreases in the afternoon due to high PV penetration, leading to a major "duck curve" profile (Fig. 17 (a)).

The HEB_I type homes with improved insulation contribute to residential load reduction. From Fig. 17 (a), it can be seen that even when as few as 25% of the houses are of the HEB_I type, the power usage reduces substantially. From Fig. 17 (b), a similarity can be observed for the studied

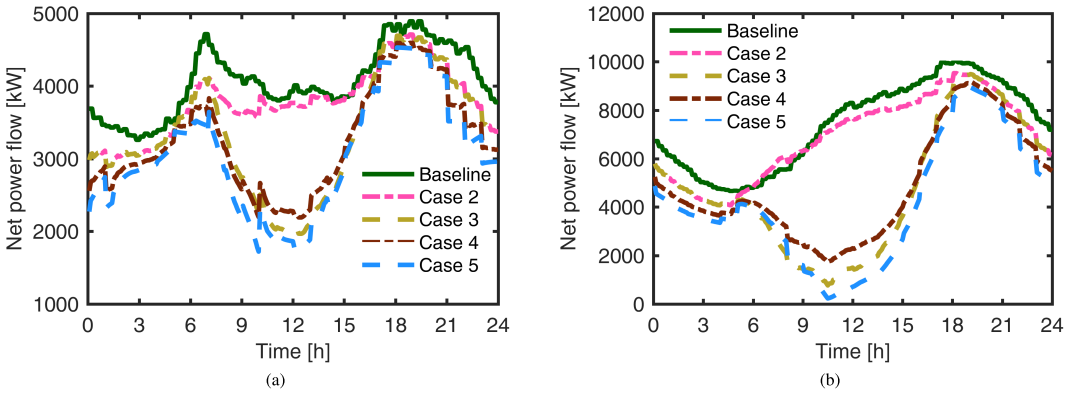


**FIGURE 17.** Aggregated residential net power flow without HEM for the studied (a) winter and (b) summer day, respectively. A high penetration of solar PV exacerbates the "duck curve".

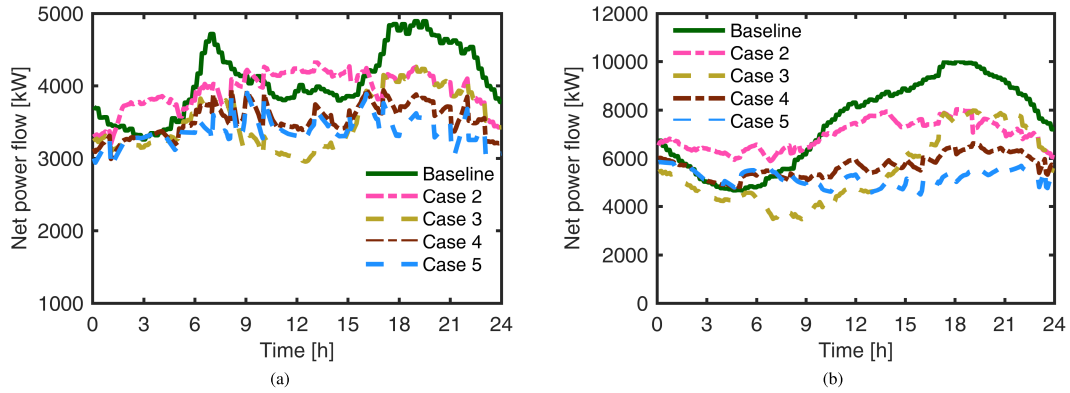


**FIGURE 18.** Aggregated residential net power flow with HEM for the studied (a) winter and (b) summer day, respectively. The proposed HEM reduces the peak demand and alleviates the "duck curve" effect.

summer day as well. The SET homes function like thermal and electrical energy storage systems with the proposed HEM control, which reduces the peak power flow in the morning and the evening in both cases as shown in 18 (a)). HEB_I homes featured in case 2, have lower energy usage compared with the baseline case, even though they do not accommodate any PV generation. Case 2 with 50% penetration of SET homes, allows the opportunity to shift the peaks and bring down the ramp rates due to the combined operation of the BESS, and the controllable HVAC and EWH loads. On the other hand, 50% penetration of SET homes having the energy storage capacity supported by controllable loads and BESS is not sufficient for case 3 to absorb all the surplus PV generation and supply the total evening demand. Hence, case 3 demonstrates a significant "duck curve" effect. In case 4, the "duck curve" effect is alleviated to a certain extent due to the combined effects of a higher percentage of SET homes and reduced PV penetrations.

The PV generation from case 5 is similar to case 3, however, case 5 requires 100% SET homes in the power system. It is noteworthy that, the power usage, peak demand, and peak to peak value for case 5 features the lowest values. The study carried out on the summar day (7/20/2017) can also be explained by applying similar observations, as shown in Fig. 18 (b). The above results clarify that high PV penetration would not form any challenges for the utility grid with the usage of appropriate HEM systems.

## VII. CONCLUSION

A co-simulation framework is developed in this article to analyze one of the largest rural field demonstrators for smart energy technologies, which is situated in Glasgow, KY, US. The community comprises more than 5,000 residential homes with 300+ smart homes along with additional business and industrial sectors. The simulated and the experimental data obtained from the case studies presented in this article demonstrate the declining trend of total power demand with the long-term growth of high PV penetration in smart homes. This study also highlights the case studies for SET smart homes that utilize solar PV, and cause the "duck curve". In this article, a smart HEM system is proposed with an aim to reduce residential peak demand by carrying out a combined optimal control of the EWH and HVAC set points. The aggregated residential load in long term is predicted in this article based on different penetrations of smart homes in a community.

The capability of EWH to provide ancillary services was studied based on the experimental data from 148 smart homes, including the net power flow from the grid, power and SOC of BESS for each house. The EWHs achieved peak

reduction at the aggregated level by shaving the water heating load while maintaining the tank temperature at acceptable levels. The minimum participation rates of EWH and BESS were calculated and compared. This article demonstrates that EWH is an attractive candidate for providing ancillary services, especially considering its near ubiquity and relatively low additional cost.

## ACKNOWLEDGMENT

Vandana Rallabandi was with the SPARK Laboratory, ECE Department, University of Kentucky, Lexington, KY 40506, USA. The authors are thankful to the Glasgow Electric Plant Board (EPB) for the example experimental data provided.

## REFERENCES

[1] F. Blaabjerg and D. M. Ionel, *Renewable Energy Devices and Systems With Simulations in MATLAB and Ansys*. Boca Raton, FL, USA: CRC Press, 2017.
[2] M. Stoyanova, Y. Nikoloudakis, S. Panagiotakis, E. Pallis, and E. K. Markakis, "A survey on the Internet of Things (IoT) forensics: Challenges, approaches, and open issues," *IEEE Commun. Surveys Tuts.*, vol. 22, no. 2, pp. 1191–1221, 2nd Quart., 2020.
[3] M. Masera, E. F. Bompard, F. Profumo, and N. Hadjsaid, "Smart (Electricity) grids for smart cities: Assessing roles and societal impacts," *Proc. IEEE*, vol. 106, no. 4, pp. 613–625, Apr. 2018.
[4] U. Zafar, S. Bayhan, and A. Sanfilippo, "Home energy management system concepts, configurations, and technologies for the smart grid," *IEEE Access*, vol. 8, pp. 119271–119286, 2020.
[5] F. Luo, G. Ranzi, C. Wan, Z. Xu, and Z. Y. Dong, "A multistage home energy management system with residential photovoltaic penetration," *IEEE Trans. Ind. Informat.*, vol. 15, no. 1, pp. 116–126, Jan. 2019.
[6] F. Y. Melhem, O. Grunder, Z. Hammoudan, and N. Moubayed, "Energy management in electrical smart grid environment using robust optimization algorithm," *IEEE Trans. Ind. Appl.*, vol. 54, no. 3, pp. 2714–2726, May 2018.
[7] S. Aznavi, P. Fajri, A. Asrari, and F. Harirchi, "Realistic and intelligent management of connected storage devices in future smart homes considering energy price tag," *IEEE Trans. Ind. Appl.*, vol. 56, no. 2, pp. 1679–1689, Mar. 2020.
[8] H. Zandi and E. McKee, "RL-HEMS: Reinforcement learning based home energy management system for HVAC energy optimization," *ASHRAE Trans.*, vol. 126, no. 1, pp. 421–429, 2020.
[9] M. Javadi, A. E. Nezhad, K. Firouzi, F. Besanjideh, M. Gough, M. Lotfi, A. Anvari-Moghadam, and J. P. S. Catalao, "Optimal operation of home energy management systems in the presence of the inverter-based heating, ventilation and air conditioning system," in *Proc. IEEE Int. Conf. Environ. Electr. Eng. IEEE Ind. Commercial Power Syst. Eur. (EEEIC/I&CPS Europe)*, Jun. 2020, pp. 1–6.
[10] M. Alavy, T. Li, and J. A. Siegel, "Energy use in residential buildings: Analyses of high-efficiency filters and HVAC fans," *Energy Buildings*, vol. 209, Feb. 2020, Art. no. 109697.
[11] R. Z. Homod, K. S. Gaeid, S. M. Dawood, A. Hatami, and K. S. Sahari, "Evaluation of energy-saving potential for optimal time response of HVAC control system in smart buildings," *Appl. Energy*, vol. 271, Aug. 2020, Art. no. 115255.
[12] S. Khemakhem, M. Rekik, and L. Krichen, "Optimal appliances scheduling for demand response strategy in smart home," in *Proc. 18th Int. Conf. Sci. Techn. Autom. Control Comput. Eng. (STA)*, Dec. 2017, pp. 546–550.
[13] Y. Wang, X. Ai, Z. Tan, L. Yan, and S. Liu, "Interactive dispatch modes and bidding strategy of multiple virtual power plants based on demand response and game theory," *IEEE Trans. Smart Grid*, vol. 7, no. 1, pp. 510–519, Jan. 2016.
[14] G. Brusco, G. Barone, A. Burgio, D. Menniti, A. Pinnarelli, L. Scarcello, and N. Sorrentino, "A smartbox as a low-cost home automation solution for prosumers with a battery storage system in a demand response program," in *Proc. IEEE 16th Int. Conf. Environ. Electr. Eng. (EEEIC)*, Jun. 2016, pp. 1–6.
[15] L. Bhamidi and S. Sivasubramani, "Optimal sizing of smart home renewable energy resources and battery under prosumer-based energy management," *IEEE Syst. J.*, early access, Feb. 3, 2020, doi: 10.1109/JSYST.2020.2967351.
[16] P. Denholm, M. O'Connell, G. Brinkman, and J. Jorgenson, "Overgeneration from solar energy in California. A field guide to the duck chart," NREL, Golden, CO, USA, Tech. Rep. NREL/TP-6A20-65023, 2015.
[17] R. H. Schulte and F. C. Fletcher, "100% clean energy: The california conundrum," *Electr. J.*, vol. 32, no. 2, pp. 31–36, Mar. 2019.
[18] D. Watson and M. Rodgers, "Utility-scale storage providing peak power to displace on-island diesel generation," *J. Energy Storage*, vol. 22, pp. 80–87, Apr. 2019.
[19] *Electricity Ancillary Services Primer*. Accessed: Nov. 28, 2020. [Online]. Available: http://nescoe.com/wp-content/uploads/2017/11/AnxSvcPrimer_Sep2017.pdf
[20] H. Gong, V. Rallabandi, M. L. McIntyre, and D. M. Ionel, "On the optimal energy controls for large scale residential communities including smart homes," in *Proc. IEEE Energy Convers. Congr. Expo. (ECCE)*, Sep. 2019, pp. 503–507.
[21] R. El Geneidy and B. Howard, "Contracted energy flexibility characteristics of communities: Analysis of a control strategy for demand response," *Appl. Energy*, vol. 263, Apr. 2020, Art. no. 114600.
[22] X.-D. Chen, L. Li, M.-L. Tseng, K. Tan, and M. H. Ali, "Improving power quality efficient in demand response: Aggregated heating, ventilation and air-conditioning systems," *J. Cleaner Prod.*, vol. 267, Sep. 2020, Art. no. 122178.
[23] H. Gong, E. S. Jones, R. E. Alden, A. G. Frye, D. Colliver, and D. M. Ionel, "Demand response of HVACs in large residential communities based on experimental developments," in *Proc. IEEE Energy Convers. Congr. Expo. (ECCE)*, Oct. 2020, pp. 4545–4548.
[24] T. Peirelinck, C. Hermans, F. Spiessens, and G. Deconinck, "Domain randomization for demand response of an electric water heater," *IEEE Trans. Smart Grid*, early access, Sep. 21, 2020, doi: 10.1109/TSG.2020.3024656.
[25] *Eia Residential Energy Consumption Survey (RECS)*. Accessed: Nov. 28, 2020. [Online]. Available: https://www.eia.gov/consumption/residential/data/2015/#waterheating
[26] M. T. Beyerle and J. D. Nelson, "Water heater with integral thermal mixing valve assembly and method," U.S. Patent 9 268 342, Feb. 23, 2016.
[27] *Bpa Regional Study of CTA-2045 Enabled Water Heaters*. Accessed: Nov. 28, 2020. [Online]. Available: https://www.bpa.gov/EE/Technology/demand-response/Pages/CTA2045-DataShare.aspx
[28] *Filed Test Results of the Consumer Technology Association's CTA-2045 Demand Response Standard*. Accessed: Nov. 28, 2020. [Online]. Available: https://www.peakload.org/assets/35thConf/A4CTA2045PanelSession.pdf
[29] H. Gong, V. Rallabandi, D. M. Ionel, D. Colliver, S. Duerr, and C. Ababei, "Dynamic modeling and optimal design for net zero energy houses including hybrid electric and thermal energy storage," *IEEE Trans. Ind. Appl.*, vol. 56, no. 4, pp. 4102–4113, Aug. 2020.
[30] Y. Qi, D. Wang, X. Wang, H. Jia, T. Pu, N. Chen, and K. Liu, "Frequency control ancillary service provided by efficient power plants integrated in queuing-controlled domestic water heaters," *Energies*, vol. 10, no. 4, p. 559, Apr. 2017.
[31] T. Clarke, T. Slay, C. Eustis, and R. B. Bass, "Aggregation of residential water heaters for peak shifting and frequency response services," *IEEE Open Access J. Power Energy*, vol. 7, pp. 22–30, 2020.
[32] *TVA Smart Community*. Accessed: Nov. 28, 2020. [Online]. Available: https://www.tva.com/environment/environmental-stewardship/epa-mitigation-projects/smart-communities
[33] H. Gong, V. Rallabandi, D. M. Ionel, D. Colliver, S. Duerr, and C. Ababei, "Net zero energy houses with dispatchable solar PV power supported by electric water heater and battery energy storage," in *Proc. IEEE Energy Convers. Congr. Expo. (ECCE)*, Sep. 2018, pp. 2498–2503.
[34] J. H. Yoon, R. Baldick, and A. Novoselac, "Dynamic demand response controller based on real-time retail price for residential buildings," *IEEE Trans. Smart Grid*, vol. 5, no. 1, pp. 121–129, Jan. 2014.
[35] M. Pipattanasomporn, M. Kuzlu, and S. Rahman, "An algorithm for intelligent home energy management and demand response analysis," *IEEE Trans. Smart Grid*, vol. 3, no. 4, pp. 2166–2173, Dec. 2012.
[36] *Hourly Electricity Consumption Varies Throughout the Day and Across Seasons*. Accessed: Nov. 28, 2020. [Online]. Available: https://www.eia.gov/todayinenergy/detail.php?id=42915
[37] B. Cui, J. Joe, J. Munk, J. Sun, and T. Kuruganti, "Load flexibility analysis of residential HVAC and water heating and commercial refrigeration," ORNL, Oak Ridge, TN, USA, Tech. Rep. NREL/TP-6A20-65023, 2019.
[38] *Savings Project: Lower Water Heating Temperature*. "Accessed: Nov. 28, 2020. [Online]. Available: https://www.energy.gov/energysaver/services/do-it-yourself-energy-savings-projects/savings-project-lower-water-heating

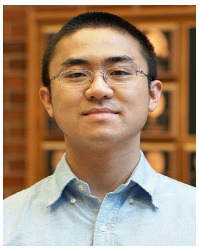

**HUANGJIE GONG** (Student Member, IEEE) received the B.Eng. degree in automation from Harbin Engineering University, Harbin, China, in 2013, and the M.S. degree in control theory and control engineering from Southwest Jiaotong University, Chengdu, China, in 2016, with a thesis on the maximum power point tracking of PV systems. He is currently pursuing the Ph.D. degree with the SPARK Laboratory, ECE Department, University of Kentucky, Lexington, KY, USA. He was a Teaching Assistant and a Research Assistant on projects sponsored by DOE, NSF, Electric Power Research Institute (EPRI), industry, and utilities. He is also the main developer of an HPC-based large-scale co-simulation software framework for energy usage in buildings and power flow in electric distribution systems incorporating EnergyPlus and OpenDSS as computational engines. His research interests include renewable energy integration, modeling, and control of energy storage, batteries, water heaters, HVAC systems, EV, net zero energy (NZE) buildings, and microgrids.

**VANDANA RALLABANDI** (Senior Member, IEEE) received the master's and Ph.D. degrees from IIT Bombay, Mumbai, India. She joined the GE Research Center upon the completion of her Ph.D. She was a Postdoctoral Researcher with the SPARK Lab, University of Kentucky, Lexington, KY, USA. She is currently a Lead Engineer with the GE Research Center, Niskayuna, NY, USA. She published more than 70 technical articles, three of which received awards from the IEEE, and one from the IET. She has coauthored four book chapters, and has more than five patent and patent pending applications. Her research interests include electric machines, power electronics drives, renewable energy devices and systems, energy storage, and power systems.

She is an Associate Editor for the IEEE TRANSACTIONS ON ENERGY CONVERSION. She has been a Reviewer for various journals and conference proceedings including the IEEE TRANSACTIONS ON INDUSTRY APPLICATIONS, the IEEE TRANSACTIONS ON ENERGY CONVERSION, the IEEE TRANSACTIONS ON POWER ELECTRONICS, the IEEE TRANSACTIONS ON POWER ELECTRONICS, and the *IEEE Transactions on Magnetics*, *IET Electric Power Applications*, and *Electric Power Components and Systems*.

**MICHAEL L. MCINTYRE** (Senior Member, IEEE) received the B.S. and M.Eng. degrees from the Department of Electrical and Computer Engineering, University of Louisville, in 1997 and 2000, respectively, and the Ph.D. degree from the Department of Electrical Engineering, Clemson University, in 2006. He was with General Electric as a Senior Electronic Design Engineer from 1998 to 2003 and then again from 2006 to 2007. He was the Kerr-Greulich Chair of energy systems with the Department of Engineering, Western Kentucky University, from 2007 to 2011. In August 2011, he joined the Electrical and Computer Engineering Department, University of Louisville, where he is currently an Associate Professor. His research interests include electrical energy systems (electronics, power electronics, and electric drive systems), control systems (linear systems, uncertain systems, and nonlinear systems), developing novel control and observation schemes for applications for electrical energy systems, electrical machinery, power electronic interfaces, renewable sources, and smart grid applications.

Dr. McIntyre is a member of numerous societies within IEEE. He is an annual reviewer of various power electronic and control systems conferences and transaction articles.

**EKLAS HOSSAIN** (Senior Member, IEEE) received the B.S. degree in electrical and electronic engineering from the Khulna University of Engineering and Technology, Bangladesh, in 2006, the M.S. degree in mechatronics and robotics engineering from the International Islamic University of Malaysia, Malaysia, in 2010, and the Ph.D. degree from the College of Engineering and Applied Science, University of Wisconsin–Milwaukee (UWM). He is currently as an Associate Researcher with the Oregon Renewable Energy Center (OREC). He is now involved with several research projects on renewable energy and grid tied microgrid system at the Oregon Institute of Technology (Oregon Tech), where he has been an Assistant Professor with the Department of Electrical Engineering and Renewable Energy since 2015. He has been working in the area of distributed power systems and renewable energy integration for last 13 years. He has published a number of research articles and posters in this field. He with his dedicated research team, is looking forward to exploring methods to make the electric power systems more sustainable, cost-effective and secure through extensive research and analysis on energy storage, microgrid systems, and renewable energy sources. His research interests include modeling, analysis, design, and control of power electronic devices; energy storage systems; renewable energy sources; integration of distributed generation systems; microgrid and smart grid applications; robotics, and advanced control systems. He is the Senior Member of the Association of Energy Engineers (AEE). He has been awarded the Faculty Achievement Award, in 2020, as the winner, the Rising Faculty Scholar Award, in 2019, as the winner, and the 2017 as the honorary mention from Oregon Institute of Technology for his outstanding contribution in teaching and research. He is currently serving as an Associate Editor for IEEE ACCESS. He is a registered Professional Engineer (PE) OR, USA. He is the Associate Editor of IEEE ACCESS, the IEEE SYSTEMS JOURNAL, and *IET Renewable Power Generation* journals. He is also a Certified Energy Manager (CEM) and Renewable Energy Professional (REP).

**DAN M. IONEL** (Fellow, IEEE) received the M.Eng. and Ph.D. degrees in electrical engineering from the Polytechnic University of Bucharest, Bucharest, Romania. His Ph.D. program included a Leverhulme Visiting Fellowship with the University of Bath, Bath, U.K., and later, he was a Postdoctoral Researcher with the SPEED Laboratory, University of Glasgow, Glasgow, U.K.

He worked in industry, most recently as a Chief Engineer with Regal Beloit Corporation, Grafton, WI, USA, and before that, as the Chief Scientist with Vestas Wind Turbines. Concurrently, he was also a Visiting and Research Professor with the University of Wisconsin and Marquette University, Milwaukee, WI, USA. He is currently a Professor of electrical engineering and the L. Stanley Pigman Chair in power with the University of Kentucky, Lexington, KY, USA, where he is also the Director of the Power and Energy Institute of Kentucky (PEIK) and of the SPARK Laboratory. He contributed to technology developments with long lasting industrial impact, holds more than 35 patents, coauthored three books, and published more than 200 articles, including seven that received IEEE awards. His research has been supported directly by industry and utilities, and by NSF, NIST, DOE, and NASA.

Dr. Ionel received the IEEE Power and Energy Society Veinott Award. He was the Inaugural Chair of the IEEE Industry Applications Society Renewable and Sustainable Energy Conversion Systems Committee, an Editor for the IEEE TRANSACTIONS ON SUSTAINABLE ENERGY, the Chair of the IEEE PES MSC and of the IEEE WG 1812, the Technical Program Chair of 2015 IEEE ECCCE, and the General Chair of the 2017 IEEE IEMDC. He is the Chair of the Steering Committee for the IEEE IEMDC Conferences. He is the Editor-in-Chief of the *Electric Power Components and Systems* journal.